journal

J. Am. Ceram. Soc., 95 [8] 2435–2438 (2012)
DOI: 10.1111/j.1551-2916.2012.05111.x

The Mechanism of Core/Shell Structure Formation During Sintering of $BaTiO_3$-Based Ceramics

Sang-Chae Jeon,[‡] Chul-Seung Lee,[§] and Suk-Joong L. Kang[‡,†,*]

[‡]Materials Interface Laboratory, Department of Materials Science and Engineering, Korea Advanced Institute of Science and Technology, 291 Daehak-ro, Yuseong-gu Daejeon 305-701, Korea

[§]LCR Division, Samsung Electro-Mechanics, Suwon 443-743, Korea

The mechanism of core/shell formation during sintering in $BaTiO_3$-based systems was studied in (Mg, Y)-doped $BaTiO_3$. The effect of ball milling time on core size and shell thickness was first observed. The core size was similar irrespective of ball milling time whereas the shell thickness increased with increasing ball milling time. The measured powder size after ball milling suggested that the cores were from the larger $BaTiO_3$ particles and the shells formed via dissolution of smaller particles and precipitation of dissolved material, in contrast with the interpretation of the results of a previous investigation. To identify the core/shell formation mechanism, bi-layer samples with different chemical compositions, $94BaTiO_3$–$2Y_2O_3$–2MgO–$2SiO_2$ (mol%) (BT–YMS) and $98BaTiO_3$–$2SiO_2$ (mol%) (BT–S), and different grain sizes were prepared. The morphology of the newly formed shell layer and the shape of an {111} twin across the interface between a core and a shell confirmed that the formation mechanism of the core/shell structure during sintering is the dissolution and precipitation of material rather than solid-state diffusion of solutes into $BaTiO_3$.

I. Introduction

In the application of $BaTiO_3$-based ceramics as dielectric materials, including multilayer ceramic capacitors (MLCCs) in particular, the temperature dependence of the dielectric properties should be minimized.[1,2] One approach to achieve this objective is producing $BaTiO_3$ grains with a core/shell structure–a core of pure $BaTiO_3$ and a shell comprising a solid solution of $BaTiO_3$ with solute elements.[3–7] A $BaTiO_3$ grain with a core/shell structure consists of a tetragonal ferroelectric core covered with a paraelectric pseudocubic shell at the temperature of use. The core exhibits high dielectric permittivity with a peak value at the Curie temperature (T_C) whereas the shell has low dielectric permittivity above room temperature. The overall dielectric behavior exhibits an insensitive dielectric response to temperature variation, showing diffuse phase transition (DPT) behavior.[1]

As the first report on the formation of a core/shell structure in Nb-added $BaTiO_3$,[3] the formation of a core/shell structure in $BaTiO_3$ has been a key issue in both academic and industrial circles. With respect to technological considerations, proper control of the core/shell structure via the use of appropriate dopants has been an issue to produce capacitors for a wide temperature range of application. In academia, many investigations have been carried out to gain understanding of the formation mechanism of the core/shell structure. To date, two mechanisms have been proposed: an inter-lattice diffusion mechanism[8,9] and a dissolution/precipitation mechanism.[5,10] According to the former, the shell forms via solid-state diffusion of dopants into $BaTiO_3$ particles. In contrast, the dissolution/precipitation mechanism considers the formation of the shell to be a result of the precipitation of dopants containing $BaTiO_3$ from the liquid matrix. As outlined above, consensus on the formation mechanism has remained elusive.

The purpose of this study is to demonstrate the formation mechanism of the core/shell structure through a model experiment using diffusion couples. Through careful observation of a new solid solution layer formed on large $BaTiO_3$ grains near the interface between a large-grained $BaTiO_3$ sample and a sample contained small grained dopants, it was possible to easily observe the shell formation and hence to confirm the mechanism of shell formation.

II. Experimental Procedure

Samples with a composition of $94BaTiO_3$–$2Y_2O_3$–2MgO–$2SiO_2$ (mol%) (BT–YMS) and $98BaTiO_3$–$2SiO_2$ (mol%) (BT–S) were prepared using commercial powders of $BaTiO_3$ (1.4 μm, 99.6% purity, Fuji Titanium, Kanagawa, Japan), Y_2O_3 (99.9% purity, Kojundo Chemical Laboratory Co., Ltd., Saitama, Japan), MgO (99.9% purity, Ube Material Industries, Ltd., Ube, Japan), and SiO_2 (99.85% purity, Wako Pure Chemical Industries, Ltd., Osaka, Japan). To enable observation of the core/shell structure under SEM, coarse $BaTiO_3$ raw powder of 1.4 μm size was used. The composition of the BT–YMS samples was selected under consideration of the results of previous investigations where a core/shell structure formed with the addition of rare earth elements together with Mg.[8,11,12]

Two sets of experiments were performed. We first reexamined the effect of ball milling on the formation of core/shell structures. A powder mixture of the BT–YMS composition was ball-milled in high purity ethanol for different periods of time (6, 12, and 48 h) using a polypropylene bottle and zirconia balls. The dried slurry was sieved to 125 μm and lightly pressed into cylindrical pellets of 7 mm diameter and 2 mm thickness. The pellets were cold isostatically pressed at 200 MPa and were sintered at 1300°C for 1 h in wet H_2 ($P_{O2} = 10^{-13}$–10^{-14} atm). The sintering conditions were optimized to reveal differences in microstructure, in particular, average grain size.

In the second set of experiments, model experiments were performed using BT–YMS/BT–S bi-layer samples. The preparation procedure of powder pellets was the same as that in the first set. BT–YMS samples were sintered at 1350°C in wet H_2 ($P_{O2} = 10^{-13}$–10^{-14} atm) for 2 h to produce core/shell grains of small sizes. BT–S samples were sintered at

E. Olevsky—contributing editor

Manuscript No. 30556. Received October 26, 2011; approved January 17, 2012.
This work was presented at the International Conference on Sintering 2011, Jeju, Korea, Aug 31, 2011 (Sintering of electronic materials, Paper No. WeP55).
*Member, The American Ceramic Society.
†Author to whom correspondence should be addressed. e-mail: sjkang@kaist.ac.kr

1350°C in wet H_2 for 8 h to obtain large grains of 50 μm average size, which facilitated observation of the shells formed on them. The two kinds of sintered samples (BT–YMS and BT–S) were polished and joined together using glue to make a bi-layer. The bi-layer samples were embedded in $BaTiO_3$ powder and lightly pressed and then cold isostatically pressed at 200 MPa. The powder compacts containing bi-layers were annealed at 1350°C for various times in wet H_2. Diffusion bonding occurred at the interface of the bi-layer samples during annealing.

The microstructures of the samples were observed along their vertical sections using Scanning Electron Microscopy after polishing and chemical etching in a $95H_2O$–4HCl–1HF (vol.%) solution. The samples were also observed under a Transmission Electron Microscope (TEM; JEOL Ltd., Tokyo, Japan) operated at 200 kV. TEM samples were prepared by the conventional TEM sample preparation method: grinding, dimpling, and ion milling for electron transparency. The chemical compositions in different regions were measured using an Energy-Dispersive X-ray Spectroscope (STEM/EDS) attached to the TEM and also by an Electron Probe Micro Analyzer (EPMA, Shimadzu, Kyoto, Japan).

III. Results and Discussion

Figures 1(a) and (b) are SEM and TEM micrographs, respectively, showing a core/shell structure formed in the BT–YMS sample sintered at 1350°C for 2 h in wet H_2. A core/shell structure is clearly revealed by SEM after proper etching of the sample. In Fig. 1(b), a tetragonal core region with a well-developed domain structure is distinguished from a pseudo-cubic shell region with no domain structure. The electron-diffraction patterns from the core and the shell shown in Fig. 1(b) indicate that they have the same crystallographic orientation as reported in a previous investigation.[13] The interface between the core and the shell observed under HRTEM (High-Resolution TEM) in Fig. 1(c) also confirms crystallographic coherency at the core/shell boundary, as reported previously.[14] The distributions of dopants measured by STEM/EDS in Fig. 1(d) for a core and a shell show the practical absence of Y in the core whereas the presence of an appreciable amount of Y in the shell is noted. On the other hand, a small amount of Mg is detected both in the core and in the shell, possibly due to the difficulty in exactly measuring Mg concentration by STEM/EDS.[12] The present TEM micrographs and STEM/EDS results are in agreement with those obtained in a previous study of the $BaTiO_3$–MgO–Y_2O_3 system.[12]

Several investigations have sought to identify the formation mechanism of the core/shell structure in doped $BaTiO_3$.[5,8–10] Wang *et al.*[9] observed the variation in core size and shell thickness with milling time. As the milling time increased, the core size became smaller and the shell thickness thicker. Nevertheless, the grain size was apparently invariable. This observation was explained as a result of a possible increase in defect concentrations in particles during milling, which in turn can promote solid-state diffusion at the surface of $BaTiO_3$. They suggested that the solid-state diffusion of Y and Mg into $BaTiO_3$ particles resulted in the formation of a shell. According to the micrographs presented in their article, however, it is apparent that grain growth occurred during sintering.

On the other hand, Randall *et al.* claimed that the formation process of a core/shell structure in LiF-doped $BaTiO_3$ entailed the dissolution of small grains into a liquid and precipitation of the dissolved materials on large grains from the liquid.[10] They suggested that a core/shell structure forms whenever a liquid phase is present and the solubility of $BaTiO_3$ in the liquid is sufficiently high. This dissolution/precipitation mechanism was also proposed to be operative in the $BaTiO_3$–$SrTiO_3$ system.[15]

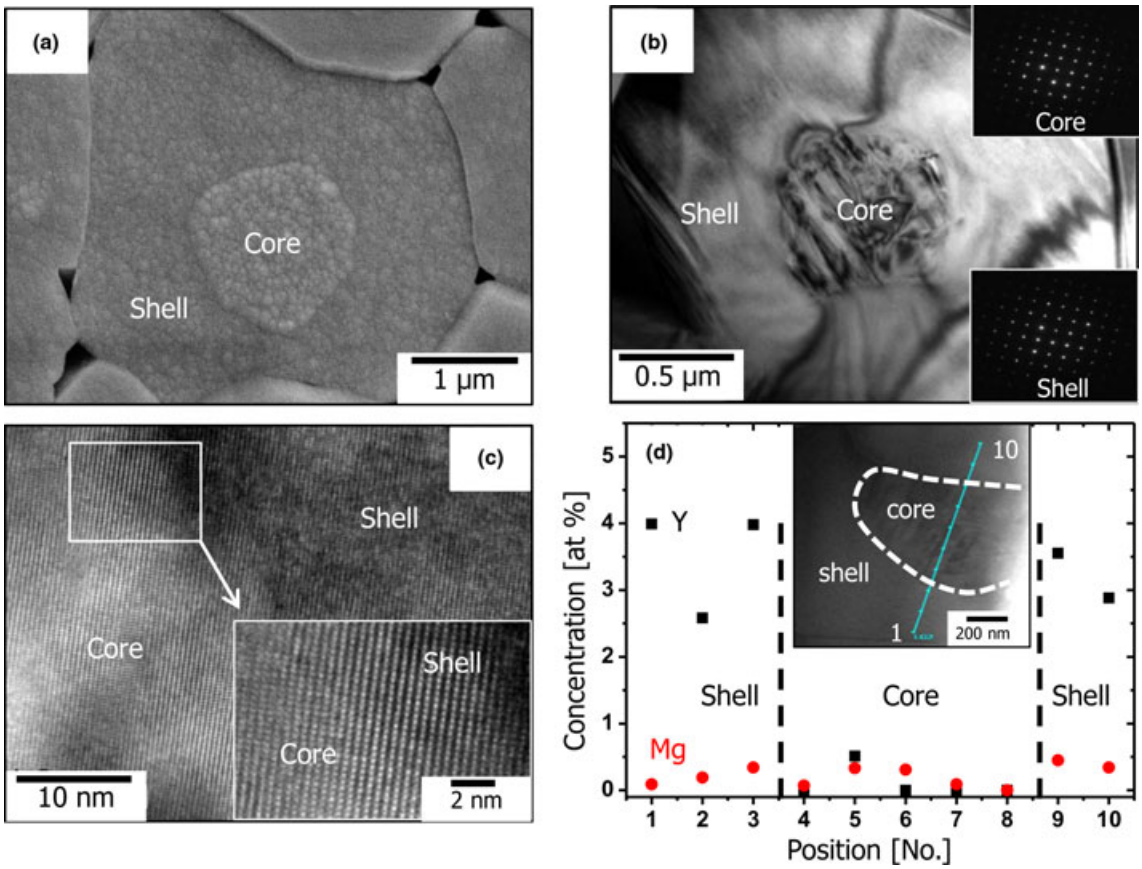

Fig. 1. (a) SEM, (b) TEM micrographs showing typical core-shell structures in a sample sintered at 1350°C in wet H_2 for 2 h, (c) a HRTEM image at the interface between a core and a shell, and (d) STEM/EDS line profile showing the distribution of Y and Mg.

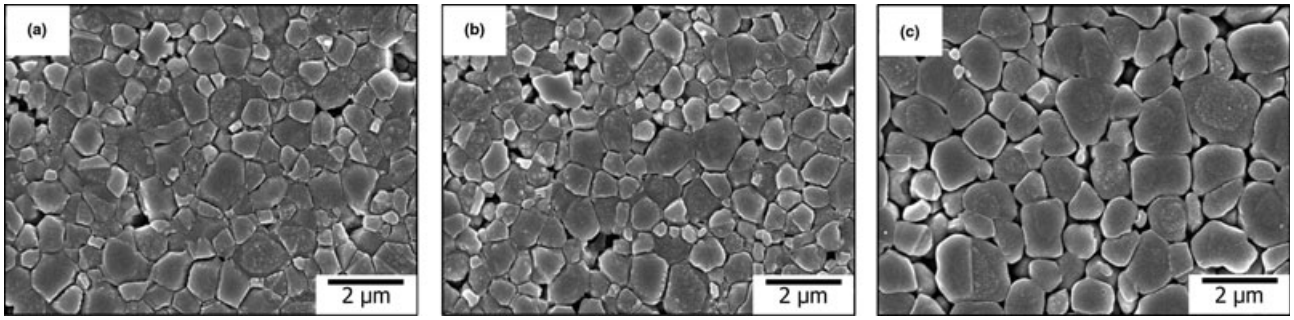

Fig. 2. SEM micrographs of BT–YMS samples sintered at 1300°C for 1 h in wet H_2 after milling for (a) 6, (b) 12, and (c) 48 h.

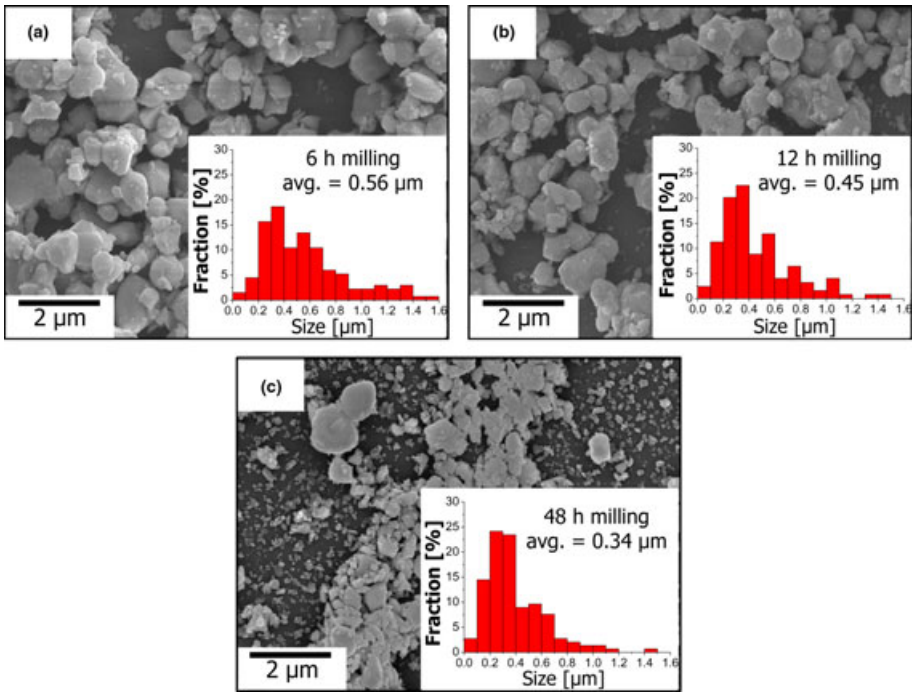

Fig. 3. SEM micrographs and size distributions of powders after ball milling for (a) 6, (b) 12, and (c) 48 h.

To evaluate the validity of the two mechanisms, i.e., solid-state diffusion and dissolution/precipitation, we first examined the ball milling effect on the formation of core/shell structures, as also carried out by Wang *et al.*[9] Figure 2 shows the microstructures of the BT–YMS samples sintered at 1300°C for 1 h in wet H_2 with different ball milling times: (a) 6, (b) 12, and (c) 48 h. The average grain size after sintering is larger for samples with longer milling time. In particular, appreciable grain growth occurred in the 48 h milled sample. In addition, thicker shell layers formed in the 48 h milled sample than in the 6 h and 12 h milled samples. However, size measurements of more than 50 cores for each sample revealed that the average core size (standard deviation) in 2-dimensional cross-sections was similar regardless of the milling time: 0.79 (0.26), 0.81 (0.21), and 0.76 (0.23) μm for 6, 12, and 48 h milling, respectively. Under the assumption that the sizes of cores in each sample were the same, the 3-dimensional size of the cores was estimated to be 1.04, 1.07, and 1.00 μm for the 6, 12, and 48 h milled samples, respectively, by dividing the 2-dimensional value by 0.76.[16] This suggests that the shells formed on cores of similar sizes during sintering, in contrast with the claim in a previous investigation.[9] To confirm the present findings, we examined the particle size distribution after ball milling.

Figure 3 shows micrographs of ball-milled powders and their measured particle size distributions. As the period of ball milling is increased, more particles are broken into small pieces, resulting in a decrease in the average particle size: 0.56, 0.45, and 0.34 μm for 6, 12, and 48 h milling, respectively. However, the sizes of the largest particles of the different samples are roughly the same, 1.5 μm, irrespective of the milling time, as shown in Fig. 3.

As the driving force for grain growth increases with decreasing average particle size, the observed increase in average grain size with increasing milling time, as seen in Fig. 2, is due to the increase in the driving force for grain growth. The similar size of cores in samples with different ball milling times, on the other hand, can be attributed to the difference in the size distribution of particles. When Ostwald ripening occurs during liquid phase sintering, large grains grow and small grains dissolve.[17] As the sizes of large particles are similar in three different samples and only large grains can remain as cores, the cores of growing grains are similar, as observed in this study. This supports the dissolution/precipitation mechanism of shell formation.

To clarify the dissolution/precipitation mechanism, a bi-layer model experiment was performed, and the results clearly show the original grain before its growth and the interface between the grain and the shell that was formed during subsequent annealing. The micrograph in Fig. 4(a) shows a well-bonded interface of the bi-layer sample of BT–S and BT–YMS. Etched micrographs of BT–S and BT–YMS samples are also shown in the two upper insets. When this bi-layer sample was annealed at 1350°C, the large grains in the BT–S sample grew into the BT–YMS sample forming a new layer, as shown in Fig. 4(b). The new layer is a shell

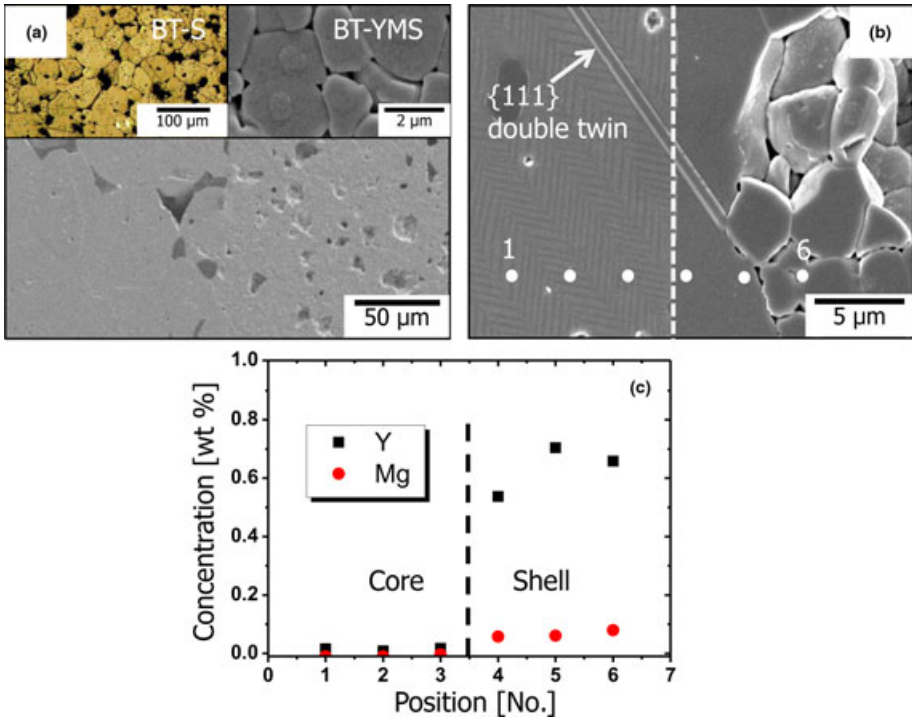

Fig. 4. (a) Microstructure showing the interface of a diffusion couple of BT–S and BT–YMS layers before annealing. Two insets in the upper part in Fig. 4(a) show the microstructures of the two diffusion layers, (b) Microstructure of the diffusion couple after annealing at 1350°C in wet H_2 for 1 h, and (c) Measured dopant concentrations across the original grain and the shell.

that contains Y and Mg, as measured in Fig. 4(c). The shell has no visible domains [Fig. 4(b)] and contains high Y concentration. In particular, the {111} double twins formed in a large grain in the BT–S sample are extended to the BT–YMS sample [Fig. 4(b)], indicating that the layer grew epitaxially by dissolution of small grains and precipitation of the dissolved material onto the growing grains. These results clearly demonstrate that the formation mechanism of the core/shell structure in $BaTiO_3$ is dissolution/precipitation rather than solid-state diffusion, in support of some previous works.[5,10]

IV. Conclusion

The formation mechanism of the core/shell structure in $BaTiO_3$ has been revisited. An experiment to evaluate the ball-milling effect showed that the core size was similar irrespective of ball milling time whereas the average grain size increased with ball milling time. These results were related to the difference in the size distribution of particles after ball milling. They also supported the dissolution/precipitation mechanism of shell formation. A bi-layer experiment with coarse and fine grains with different chemical compositions revealed that a shell layer formed on large grains, with their growth toward fine grains, confirming the dissolution/precipitation mechanism. It is concluded that the mechanism of shell formation in $BaTiO_3$-based ceramics is dissolution/precipitation of the material during sintering. This conclusion may lend insight into processing conditions for optimization of core/shell structures in $BaTiO_3$-based ceramics.

V. Acknowledgments

This work was supported by Samsung Electro-Mechanics Co. Ltd. through the Center for Advanced MLCC Manufacturing Processes and also by a National Research Foundation of Korea (NRF) grant funded by the Korean government (MEST) (No. 2011-0017556).

References

[1]D. Hennings, "Barium Titanate Based Ceramic Materials for Dielectric Use," *Int. J. High Tech. Ceram.*, **3**, 91–111 (1986).

[2]Y. Park and H. G. Kim, "Dielectric Temperature Characteristics of Cerium-Modified Barium Titanate Based Ceramics with Core-Shell Grain Structure," *J. Am. Ceram. Soc.*, **80** [1] 106–12 (1997).

[3]M. Kahn, "Effects of Sintering and Grain Growth on the Distribution of Niobium Addtion in Barium Titanate Ceramics," Ph.D. Thesis, Pennsylvania State University, University Park, PA, 1969.

[4]B. S. Rawal, M. Kahn, and W. R. Buessem, "Grain Core–Grain Shell Structure in Barium Titanate-Based Dielectrics"; pp. 172–88 in *Advances in Ceramics, Vol. 1, Grain Boundary Phenomena in Electronic Ceramics*. Edited by L. M. Levinson. American Ceramic Society, Columbus, OH, 1981.

[5]D. Hennings and G. Rosenstein, "Temperature-Stable Dielectrics Based on Chemically Inhomogeneous $BaTiO_3$," *J. Am. Ceram. Soc.*, **67** [4] 249–54 (1984).

[6]H. Y. Lu, J. S. Bow, and W. H. Deng, "Core–Shell Structures in ZrO_2-Modified $BaTiO_3$ Ceramic," *J. Am. Ceram. Soc.*, **73** [12] 3562–8 (1990).

[7]H. Chazono and M. Fujimoto, "Sintering Characteristics and Formation Mechanisms of 'Core-Shell' Structure in $BaTiO_3$-Nb_2O_5-Co_3O_5 Ternary System," *Jpn. J. Appl. Phys.*, **34**, 5354–9 (1995).

[8]H. Kishi, Y. Okino, M. Honda, Y. Iguchi, M. Imaeda, Y. Takahashi, H. Ohsato, and T. Okuda, "The Effect of MgO and Rare-Earth Oxide on Formation Behavior of Core-Shell Structure in $BaTiO_3$," *Jpn. J. Appl. Phys.*, **36**, 5954–7 (1997).

[9]T. Wang, X. H. Wang, H. Wen, and L. T. Li, "Effect of Milling Process on the Core-Shell Structures and Dielectric Properties of Fine-Grained $BaTiO_3$-Based X7R Ceramic Materials," *Int. J. Miner. Metall. Mater.*, **16**, 345–8 (2009).

[10]C. A. Randall, S. F. Wang, D. Laubscher, J. P. Dougherty, and W. Huebner, "Structure Property Relationships in Core-Shell $BaTiO_3$-LiF Ceramics," *J. Mater. Res.*, **8** [87] 1–79 (1993).

[11]C. S. Chen, C. C. Chou, W. C. Yang, and I. N. Lin, "TEM Microstructures of X7R Type Base-Metal-Electroded $BaTiO_3$ Capacitor Materials Co-Doped with MgO/Y_2O_3 Additives," *Ferroelectrics*, **332**, 41–4 (2006).

[12]C. H. Kim, K. J. Park, Y. J. Yoon, M. H. Hong, J. O. Hong and K. H. Hur, "Role of Yttrium and Magnesium in the Formation of Core-Shell Structure of $BaTiO_3$ Grains in MLCC," *J. Eur. Ceram. Soc.*, **28**, 1213–9 (2008).

[13]T. R. Armstrong and R. C. Buchanan, "Influence of Core-Shell Grains on the Internal Stress State and Permittivity Response of Zirconia-Modified Barium Titanate," *J. Am. Ceram. Soc.*, **73** [5] 1268–73 (1990).

[14]Y. C. Wu, H. Y. Lu, D. E. McCauley, and M. S. H. Chu, "The {111}-Modulated Domains in Tetragonal $BaTiO_3$," *J. Am. Ceram. Soc.*, **89** [9] 2702–9 (2006).

[15]J. S. Kim and S.-J. L. Kang, "Formation of Core-Shell Structure in the $BaTiO_3$-$SrTiO_3$ System," *J. Am. Ceram. Soc.*, **82** [4] 1085–8 (1999).

[16]W. Schatt and K. P. Wieters, *Powder Metallurgy*. European Powder Metallurgy Association, Shrewsbury, UK, 1997.

[17]S.-J. L. Kang, *Sintering: Densification, Grain Growth and Microstructure*. Elsevier Butterworth-Heinemann, Oxford, UK, 2005. □